European Journal of Pharmaceutics and Biopharmaceutics 78 (2011) 522–530

Contents lists available at ScienceDirect

European Journal of Pharmaceutics and Biopharmaceutics

journal homepage: www.elsevier.com/locate/ejpb

Research paper

Volume to dissolve applied dose (VDAD) and apparent dissolution rate (ADR): Tools to predict *in vivo* bioavailability from orally applied drug suspensions

Uwe Muenster *, Christian Pelzetter, Thomas Backensfeld, Andreas Ohm, Thomas Kuhlmann, Hartwig Mueller, Klemens Lustig, Jörg Keldenich, Susanne Greschat, Andreas H. Göller, Mark Jean Gnoth

Bayer Healthcare, Global Drug Discovery, Germany

ARTICLE INFO

Article history:
Received 19 August 2010
Accepted in revised form 31 January 2011
Available online 16 February 2011

Keywords:
Solubility
Dissolution
Bioavailability
Absorption
Development

ABSTRACT

Low solubility of drug candidates generated in research contributes to their elimination during subsequent development due to insufficient oral bioavailability (BA) of crystalline compound. Therefore, the purpose of the study was to identify critical *in vitro* solubility and dissolution parameter that would predict critical *in vivo* dissolution by means of *in vitro–in vivo* correlation. Thermodynamic solubility and apparent dissolution rate (ADR) were determined using the shake-flask method and mini-flow-through-cell, respectively. Oral BA studies in rats and humans were conducted from drug solution and suspension/tablets. Relative BA was calculated using F_{rel} [%] = $AUC_{suspension}/AUC_{solution} * 100$, representing a measure of *in vivo* dissolution. Roughly, F_{rel} rat >50% translates into F_{rel} human of >90%. Both, ADR and log volume to dissolve applied dose (VDAD), when plotted against F_{rel} rat, revealed certain threshold levels, (ADR, ~150–200 μg of compound dissolved under respective assay conditions; VDAD, ~100–500 ml/kg) which translate into F_{rel} in rats of >50%.

Thus, assuming that F_{rel} > 50% in rats is indicative of sufficient *in vivo* dissolution in humans after oral application, drugs should exhibit a VDAD of ~100–500 ml/kg or less in aqueous media to avoid insufficient or varying drug absorption.

1. Introduction

In vitro high-throughput screening (HTS) procedures in drug discovery very often generate drug candidates of poor aqueous solubility, thereby contributing to impaired oral bioavailability, increase in food effect, higher variability in pharmacokinetics, and thus to increasing patient numbers during clinical trials, which altogether lead to high attrition rates during development [1–3]. Since the *in vitro* HTS era took off in the early 1990s [4,5], hits depend no longer on sufficient solubility for *in vivo* activity, but mainly on the relation between active pharmaceutical ingredient (API) structure and *in vitro* activity. One of the most effective strategies in medicinal chemistry to improve biological activity of a compound is to add properly positioned lipophilic groups to the molecule [6]. Therefore, in many cases, an improved receptor or enzyme binding affinity is accompanied by impaired aqueous thermodynamic solubility. During the research phase, this is not critical because in HTS assays, compounds are usually added as solution to respective wells from a dimethyl sulfoxide (DMSO) stock. In such setups, the dissolved amount of API is reflected by its kinetic solubility (solubility at start of compound precipitation from supersaturated solution) under respective assay conditions and not by the APIś thermodynamic solubility (equilibrium solubility of compound in a saturated solution). As a consequence, poor thermodynamic solubility is usually not an issue during research. However, in subsequent development, it is this very thermodynamic solubility that is of utmost importance for the dissolution of the compound in the gastrointestinal (GI) tract after oral administration of a standard immediate release tablet, and thus is one factor that determines the oral bioavailability [7,8]. Therefore, during recent years, the pharmaceutical industry has been more and more confronted with a situation in which research has built-up pharmacologically highly valuable pipelines, which

Abbreviations: ADR, apparent dissolution rate; API, active pharmaceutical ingredient; AUC, area under the curve; AUC_{norm}, dose-normalized area under the curve; BA (F), bioavailability; BCS, biopharmaceutical classification system; D_0, dose strength/250 ml/solubility; DMSO, dimethyl sulfoxide; DSC, differential scanning calorimetry; F_{abs}, fraction dose absorbed; FDA, food and drug administration; F_{rel}, relative bioavailability ($F_{suspension}/F_{solution} * 100$); GI, gastrointestinal; OECD, organization for economic cooperation and development; P_{app}, apparent permeation coefficient; PEG, polyethylene glycol; USP, United States Pharmacopoe; VDAD, volume to dissolve applied dose; XRPD, X-ray powder diffraction.

* Corresponding author. Bayer Healthcare, Department Early Development, Building 456, Room 154, Aprather Weg 18a, 42096 Wuppertal, Germany. Tel.: +49 202 364837.

E-mail address: uwe.muenster@bayer.com (U. Muenster).

0939-6411/$ - see front matter © 2011 Elsevier B.V. All rights reserved.
doi:10.1016/j.ejpb.2011.01.023

are packed with compounds of poor aqueous solubility [9]. It is the authors' own experience that weak thermodynamic solubility and poor dissolution behavior resulted in either insufficient drug exposure during animal toxicology studies or insufficient absorption after oral administration to humans during clinical trials (not published). Sometimes, even severe formulation efforts – e.g., development of amorphous [10] or self-micro-emulsifying systems [11] – were not able to overcome low solubility-related bioavailability issues. Therefore, an early thermodynamic solubility assessment and elimination of poorly soluble compounds during the late research phase is desirable. Also, once critical solubility and apparent dissolution ranges have been defined, further chemical optimization may be supported by thermodynamic solubility and/or apparent dissolution data. In an attempt to describe a predictive tool for oral bioavailability from drug suspensions, apparent dissolution rates (ADR) and the logarithm of the volume to dissolve the applied dose (log VDAD, where VDAD is calculated by dividing the applied dose [mg/kg] by respective thermodynamic solubilities [mg/L] at pH 1, 4.5, and 7), were plotted against the relative bioavailability (F_{rel} [%] = dose-normalized area under the curve $(AUC_{norm})_{suspension}/(AUC_{norm})_{solution} * 100$) in rat. Results suggest certain VDAD and ADR threshold levels that should be reached in order to avoid insufficient dissolution of the compound in the GI tract when applied as solid formulation containing crystalline API.

2. Methods and materials

2.1. Test compounds and chemicals

Chemical structures of 37 compounds (named 1–37) included in the study cannot be disclosed for intellectual property reasons. However, Table 1 reveals their molecular weights, *c* log Ps [12], topological polar surface area (TPSA, [13]), pK_a for strongest acid and base [14], and mean similarities of all molecules to each single molecule expressed by Tanimoto coefficients calculated from MDL MACCS public keys ([15], Table 1). Caco-2 cells were purchased from the Deutsche Sammlung für Mikroorganismen und Zellkulturen (ACC 169, DSMZ; Braunschweig, Germany). 24-well microporous polycarbonate insert filter plates (0.4-μm pore size, Corning Costar, Inc., Cambridge, MA, USA), cell culture media, fetal bovine serum, and antibiotics were purchased from Invitrogen (GIBCO/Invitrogen, Karlsruhe, Germany). All other chemicals were purchased from Sigma Aldrich (Steinheim, Germany) and Merck (Darmstadt, Germany).

2.2. Thermodynamic solubility

Thermodynamic solubility was determined using the shake-flask method based on OECD Guideline 107 [16]. In brief,

Table 1
Physicochemical and pharmacokinetic properties of compounds.

Compound	Mol. weight	*c* log *P*	TPSA	pK_a strongest acid	pK_a strongest base	Mean similarities	Similarity referred to compound 14	P_{app} A–B (nm/s)	P_{app} B–A (nm/s)	Efflux ratio	Absolute BA (rat) (%)
1	514	5.32	94.1	–	9.04	0.58	0.63	22	23	1.0	72
2	454	2.54	88.2	10.7	–	0.54	0.56	55	456	8.3	60
3	358	4.79	50.2	−2.23	2.83	0.39	0.43	429	125	0.36	64
4	311	1.13	79.2	3.94	6.59	0.53	0.56	426	174	0.41	39
5	314	−0.49	101	6.48	3.24	0.54	0.56	40	251	6.3	26
6	527	4.67	89.5	–	7.07	0.57	0.62	42	32	0.8	79
7	554	4.17	101	8.59	11.1	0.49	0.54	67	77	1.1	28
8	526	4.92	85.3	–	7.82	0.57	0.64	13.2	5.3	0.4	62.5
9	422	1.84	138	–	4.71	0.57	0.95	38	372	9.7	49
10	378	4.11	110	10.9	6.01	0.48	0.52	255	536	2.1	94
11	460	2.80	114	11.4	3.04	0.49	0.47	130	566	4.3	106
12	400	3.23	89.1	12.9	5.10	0.51	0.51	228	606	2.7	65
13	596	5.76	138	9.16	6.89	0.54	0.63	13	542	41	20
14	408	2.84	147	10.9	4.68	0.56	1	25	237	9.5	39
15	343	2.66	88.3	13.6	1.62	0.44	0.48	311	434	1.4	62
16	474	3.21	105	–	2.24	0.48	0.46	343	487	1.4	117
17	289	2.08	88.0	13.7	1.64	0.41	0.43	90	409	4.5	42
18	483	5.18	92.4	11.4	2.94	0.49	0.54	50	21	0.41	77
19	511	5.16	123	–	4.52	0.54	0.70	19	39	2.1	25
20	539	3.26	139	–	1.49	0.47	0.45	23	554	24	31
21	414	5.98	66.0	–	2.97	0.55	0.65	7.2	2.1	0.3	74
22	436	2.39	88.0	10.7	–	0.52	0.54	76	490	6.5	55
23	649	6.36	114	7.32	–	0.43	0.43	4.8	16.8	3.5	72
24	368	6.28	49.3	10.2	6.74	0.44	0.41	192	102	0.53	95
25	512	4.40	136	–	11.6	0.54	0.73	33	18	0.61	42
26	574	5.51	106	–	3.96	0.51	0.49	1.9	1.0	0.52	92
27	520	4.47	129	–	1.57	0.49	0.52	29	0.7	0.03	42
28	534	2.99	162	13.1	–	0.50	0.53	21	9.3	0.47	44
29	676	6.38	129	10.8	5.98	0.47	0.49	4.4	215	48	38
30	420	5.53	72.6	4.64	1.35	0.43	0.39	n.a.	n.a.	n.a.	n.a.
31	520	6.88	83.9	2.99	–	0.44	0.45	29	18	0.62	51
32	443	6.87	50.2	10.8	3.8	0.56	0.63	n.a.	n.a.	n.a.	n.a.
33	443	3.96	129	12.7	7.81	0.44	0.47	n.a.	n.a.	n.a.	n.a.
34	397	2.99	95.4	–	5.19	0.52	0.76	248	139	0.56	n.a.
35	466	4.15	57.7	1.39	12.4	0.54	0.54	576	352	0.61	n.a.
36	379	5.40	59.3	8.00	4.96	0.50	0.52	n.a.	n.a.	n.a.	n.a.
37	532	6.93	67.2	10.9	7.75	0.48	0.53	n.a.	n.a.	n.a.	n.a.

n.a. = not available.
Molecular weight, calculated log *P*, topological polar surface area (TPSA), calculated pK_a for strongest acid and base, mean similarities of each molecule to all others expressed by mean Tanimoto coefficient, similarities of compound 14 to each of every other compounds expressed by Tanimoto coefficient, permeability/transport in Caco-2 cells, and absolute bioavailability in male Wistar rats of 37 research compounds.

preliminary solubility experiments in acetonitrile, dichloromethane, tetrahydrofurane, toluene, ethylacetate, acetone, 2-propanol, and methanol were conducted in order to identify appropriate crystallization solvents for each compound. A solvent was considered appropriate when approximately 10% of the compound was dissolved in a given volume. Compounds were then stirred for seven days in their respective solvents chosen for crystallization. After stirring, compounds were dried at room temperature (RT) for 72 h and analyzed for solvate formation using head-space gas chromatography (HS 40XL HS-sampler in combination with HP 5890 GC, PerkinElmer/Agilent, Rodgau-Jügesheim/Böblingen, Germany). If solvate formation occurred, stirring was repeated in a different solvent until compounds were solvate free. Then, compounds were subjected to solid state analytics. Crystallinity of the compounds was confirmed by X-ray powder diffraction (XRPD, stoe transmission diffractometer, Stoe&Cie, Darmstadt, Germany) and differential scanning calorimetry (DSC, Diamond-DSC, Perkin Elmer, Rodgau-Jügesheim, Germany). Crystalline compounds were then added in excess to aqueous media (phosphate buffer, pH 7 (United States Pharmacopoe, USP), acetate buffer, pH 4.5 (USP), 0.1 M HCl pH 1) and stirred for 16 h at 25 °C. Suspensions were centrifuged, and the supernatant as well as 1:10 and 1:100 dilutions of the supernatant were analyzed by high-performance liquid chromatography (HPLC, Agilent 1100, Agilent, Waldbronn, Germany). Appropriate analytical HPLC methods were developed upfront.

2.3. Compound micronization and particle size measurement

Compounds were micronized using an air jet mill (LSM50, high-quality steel; injector nozzle, 1.1 mm; diffuser, 3.8–5.7 mm; milling nozzle, 0.7 mm; small outlet, 9.7 mm; large outlet, 13.0 mm; injector air pressure, 4.5 bar; milling air pressure, 4.0 bar; throughput, 1 g/min; Bayer Technology, Leverkusen, Germany). In order to assess whether the micronization process had any influence on the crystallinity of the compounds, Raman spectra (RFS 100/S, Bruker, Ettlingen, Germany) and DSC curves (DSC, Diamond-DSC, Perkin Elmer, Rodgau-Jügesheim, Germany) were generated before and after micronization. Particle size of micronized compounds was determined using a Sympatec Rodos SR (Sympatec, Clausthal-Zellenfeld, Germany).

2.4. Apparent dissolution rates (ADR)

ADRs were determined using the mini-flow-through-cell ([17], USP apparatus IV, Sotax, Basel, Switzerland). One milligram of micronized compound was dispersed in glass beads, applied to the flow-through-cells, and covered with a whatman® glass microfiber filter membrane (Whatman, Kent, United Kingdom). Flow-through cells were then equilibrated to 37 °C in a water bath. Finally, a flow rate of 2 ml/min using aqueous media (phosphate citrate buffer, pH 6.8, 50 mOsm/kg; acetate buffer, pH 4.5, osmolarity, 75 mOsm/kg; 0.1 M HCl, pH 1) was applied to the flow-through-cells, and 2 min fractions of 4 ml each were collected up to 14 min after the start of the experiment. The amount of dissolved compound in each fraction was determined by HPLC (HP1100, Waldbronn, Böblingen, Germany), and apparent dissolution curves were generated.

2.5. Permeability across Caco-2 cells

Permeability across Caco-2 cell monolayers was determined as described elsewhere [18]. Briefly, Caco-2 cells were seeded at a density of 40,000 cells/well and grown for 15 days on 24-well filter insert plates with medium change every 4 days. Compounds were added at a final concentration of 2 μM to either the apical (A) or basolateral (B) compartment of insert filter plates. Compound concentrations in both the apical and basolateral (B) compartments at time points $t = 0$ h and $t = 2$ h were determined by LC–MS/MS, and respective apparent permeability coefficients (P_{app}) and efflux ratios were calculated using the following equations: (1) The apparent permeability (P_{app}) was calculated using the following equation: $P_{app} = (V_r/P_0)(1/S)(P_2/t)$, where V_r is the volume of medium in the receiver chamber, P_0 is the measured peak height or peak area of the test drug in the donor chamber at $t = 0$, S is the surface area of the monolayer, P_2 is the measured peak height or peak area of the test drug in the acceptor chamber after 2 h of incubation, and t is the incubation time. (2) Efflux ratio = P_{app} B–A/P_{app} A–B.

2.6. In vivo pharmacokinetics in humans

Human pharmacokinetic studies were carried out as single-center, randomized, open-label, non-placebo controlled, single-dose studies. Study protocols were approved by the Ethics Committee (IEC) of the North-Rhine Medical Counsil (Ethik-Kommission bei der Ärztekammer Nord-Rhein, Düsseldorf, Germany). Studies were carried out in accordance with the currently accepted declaration of Helsinki, the ICH GCP Guideline (Note for Guidance on Good Clinical Practice, and the German Drug Law (AMG)). Each subject had to confirm, in dated writing, his willingness to participate voluntarily in the trial prior to the start of the study. For determination of the relative bioavailability of 12 compounds in humans, in general, 12 healthy white male subjects (age 18–45 years, BMI 18–32 kg/m^2) received compound as an orally applied single dose, either a conventional immediate release tablet containing micronized crystalline drug substance (thus quickly providing a suspension of drug substance in the GI tract after intake) or a macrogol-based solution (polyethylene glycol (PEG) 400, 97%; Tween® 20, 2.5%; menthol, 0.5%). Compounds were administered at 8 am after overnight fasting, together with 240 ml of tap water at room temperature. The next meal was served at 1 pm. Doses differed between compounds and ranged from 2.5 to

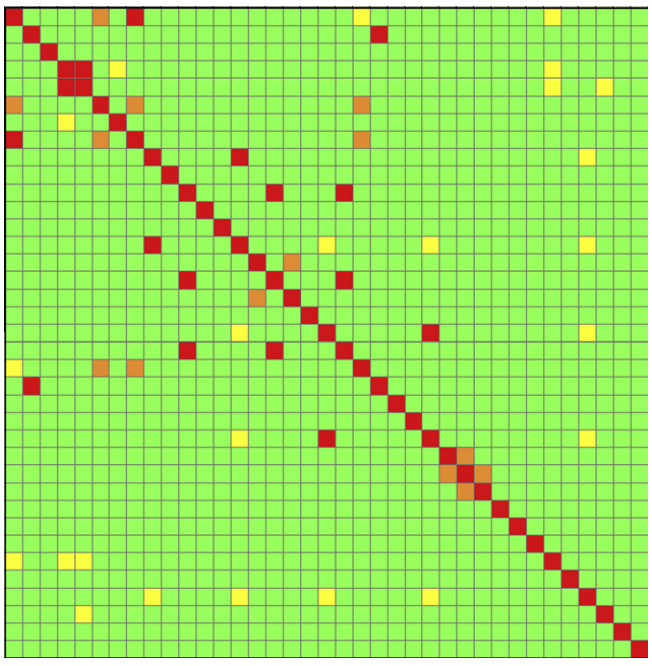

Fig. 1. Heatmap for the structural similarity of the 37 compounds calculated as pairwise Tanimoto coefficient with MDL MACCS public keys as structure fingerprint. Each cell represents the similarity of a pair of compounds with the color-coding red >0.9, orange >0.8, yellow >0.7, and green ⩽0.7.

60 mg. Blood samples were drawn over 72 h after compound application (30 min, 60 min, 90 min, 2 h, 3 h, 4 h, 6 h, 8 h, 12 h, 15 h, 24 h, 48 h, 72 h), plasma concentration–time profiles were generated, and relative bioavailability was calculated by dividing dose-normalized AUC obtained from experiments with suspension by dose-normalized AUC obtained from solution.

Table 2
P_{app} values of reference compounds in Caco-2 cells; mean of $n = 3$.

	P_{app} A–B (nm/s)	SD (nm/s)	CV (%)	BCS class based on F_{abs}	F_{abs} human (%)	References
Antipyrine	598	36	6.0	High	100	[19,20]
Caffeine	594	94	16	High	100	[21]
Carbamazipine	476	13	2.7	High	100	[19,22]
Prazosin	461	0.50	0.11	High	100	[21]
Theophylline	456	120	26.3	High	97	[19,23]
Verapamil	427	23	5.5	High	100	[19]
Ibuprofen	397	114	28.9	High	95	[21]
Propranolol	396	41	10.2	High	90	[21]
Metoprolol	325	24	7.4	High	95	[19,24]
Ketoprofen	264	67	25.3	High	100	[19,20]
Fluvastatin	175	20	11.1	High	98	[19,25]
Cimetidine	26.3	4.0	15.2	Moderate	62	[21]
Digoxin	10	0.93	9.3	Moderate	81	[19,26]
Ranitidine	15.1	1.8	12.1	Low	50	[19,24]
Hydrochlorothiazide	9.5	2.8	29	Moderate	67	[19,24]
Acyclovir	8.9	1.7	18.8	Low	30	[21]
Furosemide	6.8	7.5	11.0	Moderate	61	[19,27]
Atenolol	7.1	1.9	27	Low	50	[19,27]
Methotrexate	4.7	1.4	29.7	Low	20	[21]
Sulfasalazine	0.47	0.048	10	Low	13	[24]
Lucifer yellow	5.6	1.9	35.1		n.a.	

n.a. = not applicable.
P_{app} values of reference compounds in Caco-2 cells at 2 μM compound concentration, except digoxin and fluvastatin 50 μM, atenolol and sulfasalazine both 10 μM, after a 2-h incubation at 37 °C, were used for the validation of the Caco-2 assay (n of 3 wells per compound, for experimental details see Section 2).

Table 3
Apparent dissolution rate, thermodynamic solubility, and relative bioavailability.

Compound	Apparent dissolution rate [amount μg API dissolved after 14 min using the mini-flow-through-cell apparatus, 1 mg API per cell]			Thermodynamic solubility (mg/L)			F_{rel} at dose (% at mg/kg)
	pH 1	pH 4.5	pH 6.8	pH 1	pH 4.5	pH 7	
1	693*	753*	471	>10,000	4466	9.4	124 at 3
2	728	612	677	26	24	22	117 at 1
3	41	884*	678*	1.1	250.6	2547	106 at 0.3
4	491*	609*	648*	>10,000	1360	990	100 at 5
5	856*	838*	883*	152	136	2043	102 at 1
6	669*	773*	93	n.d.	n.d.	n.d.	100 at 16
7	721*	122	23	>10,000	215	<1	100 at 1
8	656*	38	3	n.d.	n.d.	n.d.	71 at 7
9	758*	319	198	520	15	6.0	69 at 0.3
10	786*	809	579	>10,000	47	18	65 at 1
11	113	108	106	1.8	2.1	1.6	65 at 0.3
12	428	413	400	18	19	17	59 at 3
13	753	731	803	24.1	25	23.5	59 at 1
14	839*	425	294	227	19	10	56 at 0.3
15	253	69	65	10.1	2.4	2.0	62 at 0.2
16	85	89	81	2.0	1.6	1.5	54 at 1
17	482	95	88	22.7	3.0	2.8	42 at 1
18	9	0.19	0.60	0.1	n.d	n.d.	39 at 2
19	83	0.02	0.5	2.3	<0.1	<0.1	37 at 3.8
20	46	55	43	0.9	0.9	0.9	36 at 1
21	0.1	0.1	0.3	<0.1	<0.1	<0.1	22 at 3
22	163	113	89	5	5	5	22 at 5
23	0	0	4	<1	<1	<1	16 at 0.6
24	0	16	0	<0.1	<0.1	1	13 at 15
25	83	0.5	0.7	4.3	<0.1	<0.1	5 at 5
26	0	0	0	<0.1	<0.1	<0.1	3 at 1
27	0	0.1	0.3	<1	<1	<1	2 at 5
28	0.1	0.13	0.2	<0.1	<0.1	<0.1	1 at 1
29	7	13	14	n.d.	n.d.	n.d.	0.5 at n.a.

n.a. = not available.
Apparent dissolution rate (amount API dissolved after 14 min using the mini-flow-through-cell, 1 mg API per cell; (μg), mean of $n = 2$), thermodynamic solubility (after shaking for 16 h at 25 °C, samples were drawn, centrifuged and the supernatant as well as 1:10 and 1:100 dilutions of the supernatant analyzed by HPLC, $n = 1$), and oral relative bioavailability (F_{rel}; (%), $n = 3$ for each suspension and solution) in male Wistar rats of 29 research compounds. *, bell-shaped dissolution curve (amount API dissolved after 2 min was ⩾70% of amount API dissolved after 14 min). For experimental details see Section 2.

2.7. In vivo pharmacokinetics in rat

Animals were housed and handled according to institutional guidelines issued by the government of the Federal Republic of Germany (May 25, 1998; BGBI. I S. 1105, 1818I). For the determination of pharmacokinetic parameters, male Wistar rats (Harlan Winkelmann, Borchen, Germany) were catheterized under isofluran anesthesia. One day after implantation of the catheter, compounds were administered to rats either intravenously or orally, and blood was collected into heparinized vials at various time points (three animals per time point). For intravenous administration, compounds were applied as solution in plasma containing up to 2% DMSO. Peroral vehicles contained PEG 400, ethanol, and Solutol® (ethanol/PEG400/water, 10/50/40 or ethanol/Solutol®/water, 10/20/70). The optimal vehicle was selected based on solubility data to ensure that the compounds were applied as solution. The dosing solutions were analyzed by LC–MS/MS in order to ensure that the correct doses were applied. After centrifugation, plasma was precipitated by the addition of acetonitril. The supernatants were subjected to high-performance liquid chromatography performed on an Agilent 1200 liquid chromatography system (Agilent Technologies, Waldbronn, Germany). The mobile phase consisted of 10 mM ammonium acetate (pH 3.0) and acetonitril. A linear gradient from 20% to 90% acetonitril (v/v) within 2 min was applied. Tandem mass spectrometry was performed on an API 3000 or 4000 triple-quadrupole mass spectrometer (Applied Biosystems, Darmstadt, Germany) connected to the HPLC system through a TurboIonspray interface. Pharmacokinetic parameters were calculated from plasma concentrations with Kinex, a validated *in-house* (Bayer HealthCare, Wuppertal, Germany) calculation program. For F_{rel} experiments, the dose was calculated based on the predicted effective dose in man.

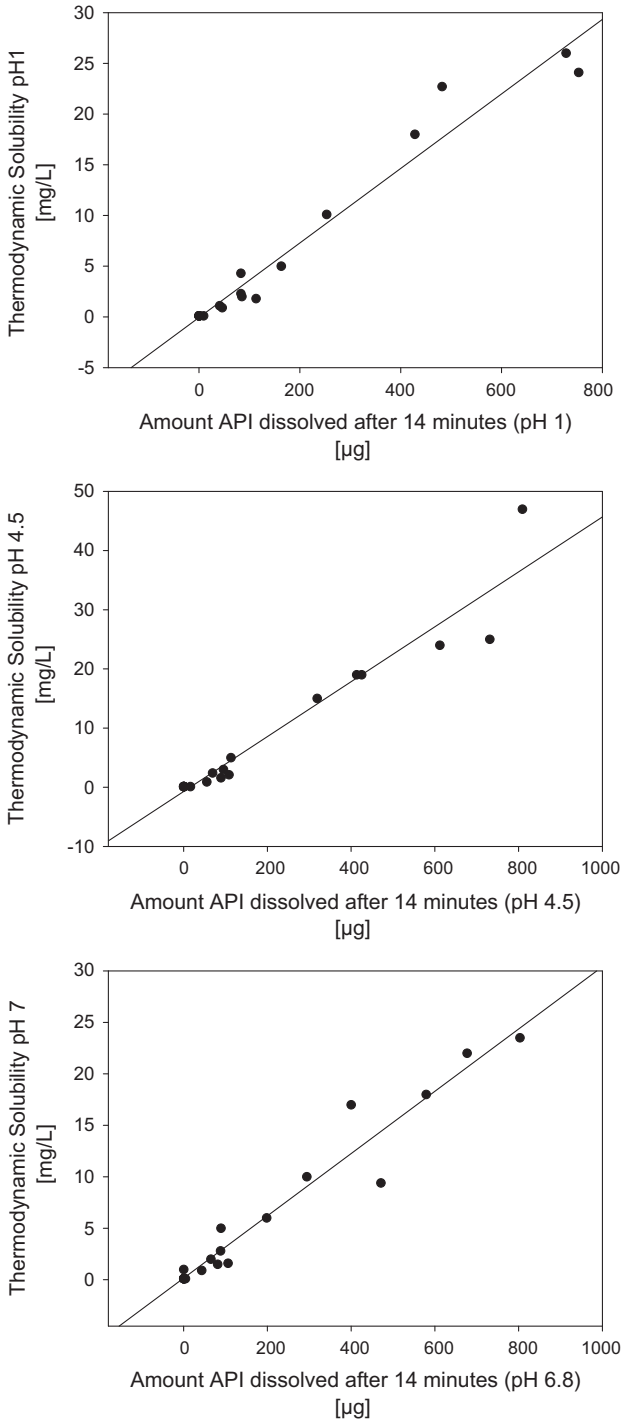

Fig. 2. Correlation of Thermodynamic Solubility (mg/L; after shaking for 16 h at 25 °C, samples were drawn, centrifuged and the supernatant as well as 1:10 and 1:100 dilutions of the supernatant analyzed by HPLC, $n = 1$) and apparent dissolution rate (amount API dissolved after 14 min using the mini-flow-through-cell, 1 mg API per cell; [µg]; mean of $n = 2$) at given pH values. Compounds that exhibited bell-shaped apparent dissolution curves (indicated with asterisk in Table 3) were not included in this correlation.

2.8. Data fitting

VDAD was calculated by dividing the applied dose [mg/kg] by respective thermodynamic solubilities [mg/L] at pH 1, 4.5, and 7. VDAD differs from the known dimensionless D_0 value (dose strength [mg/human being]/250 ml/solubility [mg/ml]) by the factor of body weight [kg] $*$ 4. The fitted curves for the log VDAD – F_{rel} correlation were created by using a sigmoidal model included in the software package WinNonlin (Version 5.0, Pharsight Corporation, Mountainview, CA).

3. Results and discussion

3.1. Physical–chemical parameter and study inclusion criteria of API

Molecular weights of the compounds were in the range of 289–676 g/mol, *c* log *P* values in the range of −0.49 to 6.93, topological

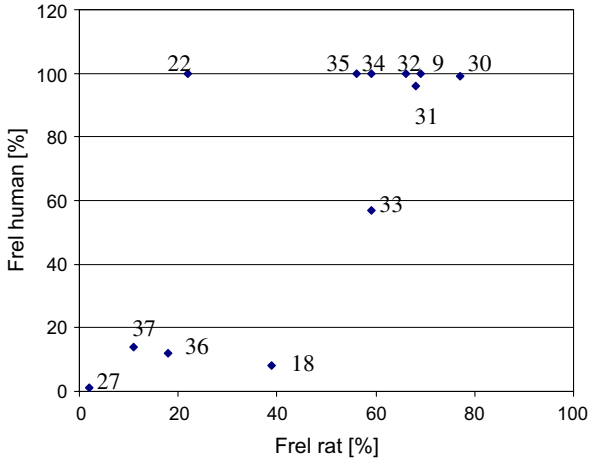

Fig. 3. Plot of relative bioavailability in male Wistar rats (AUC_{norm} from suspension/AUC_{norm} from solution $*$ 100; [%], for each formulation $n = 3$) and relative bioavailability in humans (AUC_{norm} from conventional immediate release tablet containing micronized crystalline drug substance/AUC_{norm} from solution $*$ 100; [%], for each formulation $n = 12$); compounds included are indicated by numbers (referring to Tables 1 and 3). (For interpretation of the references to color in this figure legend, the reader is referred to the web version of this article.)

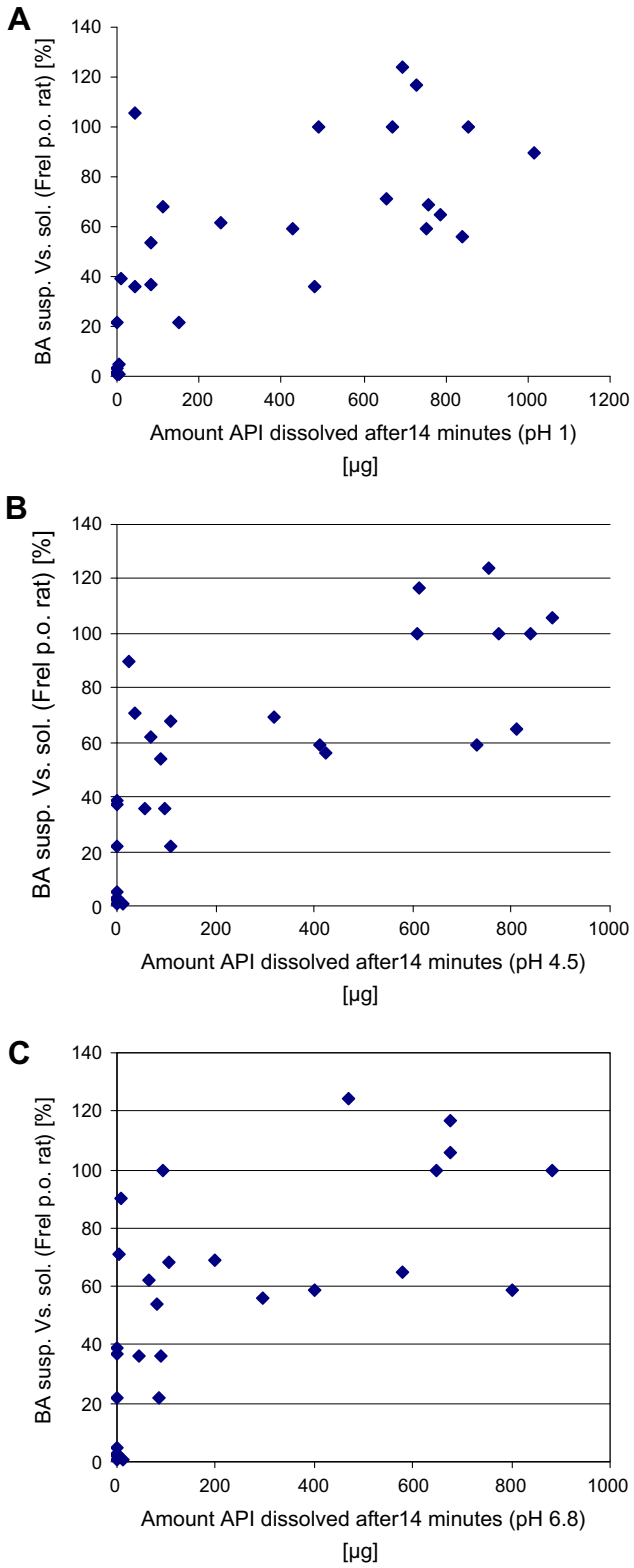

Fig. 4. Plots of apparent dissolution rate (amount API dissolved after 14 min using the mini-flow-through-cell, 1 mg API per cell; [µg]; mean of $n = 2$) at pH 1 (A), pH 4.5 (B), pH 6.8 (C), and oral relative bioavailability in male Wistar rats (oral bioavailability from suspension/oral bioavailability from solution $*$ 100; [%]; for each formulation $n = 3$) using data of compounds 1–29 presented in Table 3. (For interpretation of the references to color in this figure legend, the reader is referred to the web version of this article.)

polar surface areas (TPSA) between 49.3 and 162 Å^2, calculated pK_a values for strongest acid ranged from 0 (predicted −2.23) to no deprotonation, calculated pK_a values for strongest base ranged from 12.4 to no protonation (Table 1), altogether demonstrating physicochemical diversity of the compound set. Furthermore, as a measure for the structural diversity, we provide a heatmap in Fig. 1 where each cell represents the pairwise compound similarity of the 37 compounds calculated as pairwise Tanimoto coefficients with MDL MACCS public keys as structure fingerprints. Given that Tanimoto coefficients for structural fingerprints of lower 0.9 represent dissimilar compounds, it is clear that only eight compounds have near neighbors and the data set is structurally diverse. This is further exemplified by the very low, mean Tanimoto coefficients representing mean similarities of all molecules to each single molecule as given in Table 1 (mean similarities) and the overall mean similarities between all molecules of 0.50.

According to XRPD and DSC measurements, all compounds were crystalline after stirring for seven days in respective solvents. Particle size distribution of compounds after micronization revealed similar particle sizes in the lower micrometer range (×10 (10% fraction of particles), 0.45–1.16 µm, average 0.70 ± 0.17 µm; ×50, 1.07–5.56 µm, average 2.12 ± 0.98 µm; ×90, 2.91–12.0 µm, average 5.19 ± 2.36 µm; particle size measurement was not made with compounds 2, 9, 26, and 29). DSC and Raman measurements of samples before and after micronization showed that the micronization process had no relevant influence on the solid state of respective compounds (data not shown). In order to exclude permeation limited absorption effects *in vivo*, only compounds that show no permeation limitation were selected. According to the FDA guideline for the Biopharmaceutics Classification System [19], the Caco-2 assay can be used to estimate the fraction dose absorbed in man. To demonstrate the suitability of the Caco-2 assay, it was validated by determining P_{app} values for 20 market drugs for which the fraction dose absorbed (F_{abs}) in human subjects has been reported (Table 2, 19, 20–27). According to the FDA guideline for the Biopharmaceutics Classification System, compounds that show an F_{abs} value of >90% are classified as high permeable, compounds with an F_{abs} of 51–89% as moderate permeable, and compounds with F_{abs} values below 50% as low permeable, assuming sufficient stability within the gut (metabolism, degradation). Based on the reference compounds, a P_{app} value of >10 nm/s can be classified as moderate to high permeable (Table 2). Furthermore, the cutoff value of <10 nm/s for low-permeable compounds is in good accordance with earlier reports [28,29]. Therefore, only compounds with P_{app} A–B values of >10 nm/s were included in the study except for compounds 21, 7.2 nm/s; 23, 4.8 nm/s; 26, 1.9 nm/s; 29, 4.4 nm/s, irrespective of their efflux ratios in Caco-2 cells (Table 1). The four latter compounds were still included due to their active uptake in Caco-2 cells (compounds 21 and 26) and moderate to high absolute bioavailability of at least 20% (AUC_{norm} after oral administration/ AUC_{norm} after intravenous administration) when administered as a solution to male Wistar rats, implicating that overall pharmacokinetics is acceptable (low to moderate clearance, moderate to high permeability). Compounds with obvious permeation limitation (P_{app} < 10 nm/s and bioavailability < 20% in rat after oral application of solution) were not included in the study because such compounds are usually eliminated during the research phase and not regarded as development candidate.

3.2. In vitro determination of thermodynamic solubility and apparent dissolution rate

Thermodynamic solubilities ranged from <0.1 mg/L to >10,000 mg/L at pH 1, <0.1 mg/L to 4466 mg/L at pH 4.5, and <0.1 mg/L to 2547 mg/L (Table 3). Accordingly, amounts of API dissolved after 14 min from mini-flow-through-cells ranged between 0 µg (no detectable dissolution) and 884 µg (almost completely dissolved). As shown in Table 3, compounds with high solubility

(e.g., >10,000 mg/L at given pH) did not completely dissolve in the mini-flow-through-cell (meaning not all of the 1000 μg applied to the cell dissolved within 14 min). However, those compounds exhibited bell-shaped dissolution curves, when looking at compound concentration per fraction – time profiles (indicated with an asterisk in Table 3, indicating that the amount of API dissolved after 2 min was ⩾70% of amount of API dissolved after 14 min; yet, after 14 min, no complete dissolution was observed). Residues of highly soluble compounds in the flow-through-cell revealed that under chosen experimental conditions, those compounds may not have been completely wetted within the flow-through cells. Thermodynamic solubility correlates well with the amount of compound dissolved after 14 min in the flow-through cell apparatus at pH 1 (R^2 = 0.96), 4.5 (R^2 = 0.93), and 6.8 (R^2 = 0.95, Fig. 2A–C).

3.3. In vivo dissolution – determination of oral relative bioavailability

An adequate procedure to describe *in vivo* dissolution should be the determination of the oral relative bioavailability (F_{rel}) of a compound, meaning the dose-normalized area under the curve (AUC_{norm}) resulting from oral application of a microcrystalline drug suspension, divided by the AUC_{norm} resulting from oral application of a drug solution, multiplied by 100. This experiment, as far as possible, considers *in vivo* dissolution since all other factors influencing oral bioavailability, e.g., permeation (passive and active), drug efflux by transport proteins, metabolism should be nearly the same with suspension and solution applied. Potential drawbacks with this setup are that the compounds, especially if poorly water soluble, may precipitate in the GI tract after oral administration of the solution, which as a consequence may lead to a falsely high F_{rel}. Also, the administered vehicle, which by sense of the experiment, has to be different with solution when compared with suspension, may have an influence on oral bioavailability [30,31]. Variations in absorption and metabolism between different gut sections, as well as the influence of enterohepatic circulation cannot be dissected using this setup, rather they both are implicated in the experimental result. Further, it has to be considered that during late research, the determination of the relative bioavailability is only cost-feasible to be made in animals. Despite the beforementioned uncertainties, the F_{rel} experiment, to the best of our knowledge, represents an appropriate *in vivo* approach to collect information on *in vivo* dissolution. Thus, appropriate relative bioavailability experiments were carried out in rat and human (Table 3 and Figs. 3–5).

An F_{rel} (human) versus F_{rel} (rat) plot with a set of 12 structurally diverse (Fig. 1) compounds 9, 18, 22, 27, 30–37 (Fig. 3; only of those 12 compounds was human relative bioavailability available from respective clinical trials) leads to the assumption that a relative bioavailability of 50% in rat may be rather uncritical for compoundś *in vivo* dissolution in humans. Of the seven compounds with an F_{rel} in rat of >50%, six compounds had F_{rel} values in humans of 96–100%, one compound an F_{rel} of 57% (Fig. 3). The reason for

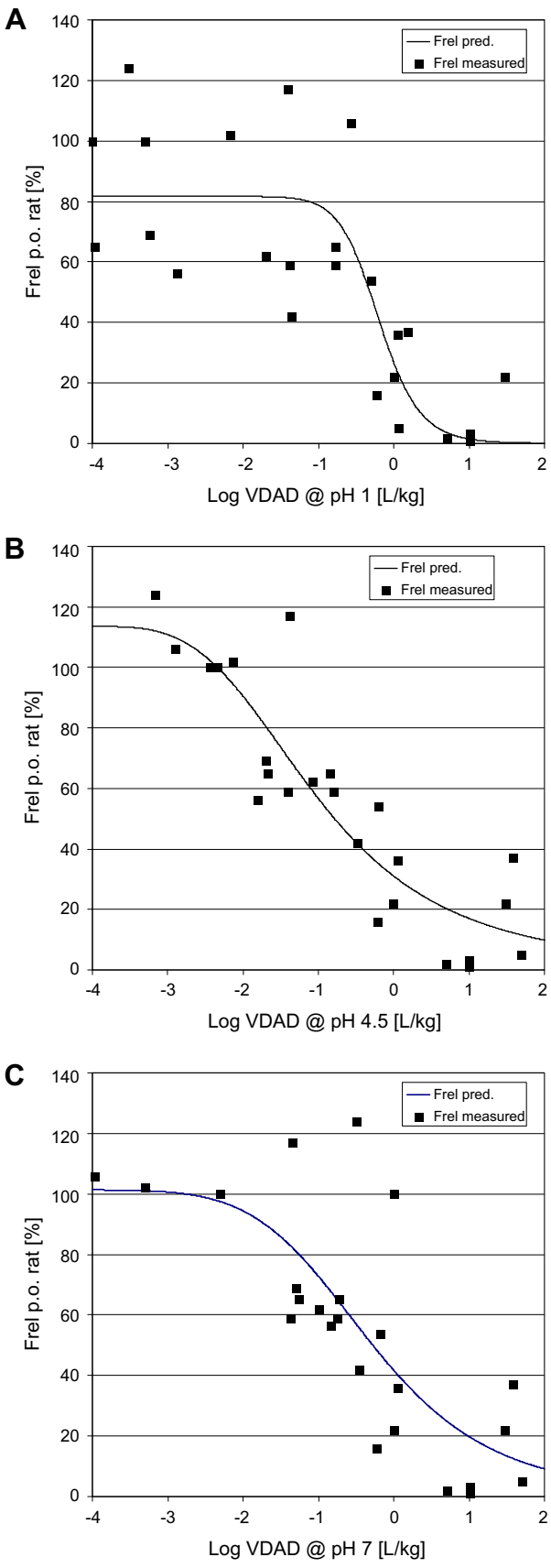

Fig. 5. Plots of log VDAD (volume to dissolve applied dose), calculated from applied dose and respective thermodynamic solubilities at pH 1 (A), pH 4.5 (B), pH 7 (C, after shaking for 16 h at 25 °C, samples were drawn, centrifuged, and the supernatant as well as 1:10 and 1:100 dilutions of the supernatant analyzed by HPLC, n = 1) [L/kg], and oral relative bioavailability in male Wistar rats (oral bioavailability from suspension/oral bioavailability from solution ∗ 100; [%], for each formulation n = 3) using data from 25 compounds presented in Table 3. Black squares, F_{rel} measured; black lines, F_{rel} predicted. Coefficients of variation [%] of the most critical parameter in the fit equations were 60%, 25%, and 40% for curve A, B, and C, respectively. A sigmoidal model was used, because the parameter F_{rel} plotted on the y axis ranged from ∼1–2% to 100% ± experimental error. The upper limit of 100% is due to the definition of F_{rel}. The lower F_{rel} limit of 1–2% is due to experimental accuracy (LOQ of LC–MS/MS analytics of blood samples). (For interpretation of the references to color in this figure legend, the reader is referred to the web version of this article.)

generally higher F_{rel} in humans when compared with rat may lie in the rat's shorter small intestinal length (rat, 0.8 m; human, 7 m) and smaller radius (rat, 0.18 cm; human, 1.75 cm) resulting in a shorter transition time (rat, 1.5 h; human, 3 h) [32–34], altogether allowing the compounds more time to dissolve in the human GI tract when compared with the rat GI tract. Thus, IR standard tablet development using crystalline API will be most likely feasible with compounds exhibiting an F_{rel} value in rat of >50% (other factors aside).

3.4. In vitro–in vivo correlations

In a next step, it was investigated whether ADR may serve as a predictor for the relative oral bioavailability of compounds whose absorption is not permeation limited (P_{app} A–B > 10 nm/s), except for compounds 21, 23, 26, and 29. Therefore, ADRs were plotted against respective relative oral bioavailabilities in rat (AUC_{norm} after p.o. application as suspension/AUC_{norm} after p.o. application as solution × 100; Fig. 4A–C). In general, relative bioavailability increased with increasing ADRs of the compounds. The ADR-dependent increase in relative bioavailability appeared to be more prominent with ADRs determined at pH 4.5 (Fig. 4B) and 6.8 (Fig. 4C), when compared with ADRs at pH 1 (Fig. 4A), probably reflecting the *in vivo* pH in rat (pH 3.8–5.0 in stomach, 6.5–7.1 in small intestine, [35]). Since all of the compounds that show ADRs of more than ~150–200 μg/14 min with either pH (except for compound 29 at pH 1), at the same time revealed F_{rel} values ⩾50%, this ADR under respective experimental conditions appears to be a rough indicator of somewhat uncritical dissolution behavior with respect to oral bioavailability from solid dosage forms.

The drawback of the F_{rel} vs. ADR plot is that it does not consider the difference in administered doses, which ranged from 0.2 mg/kg to 5 mg/kg (Table 3). Therefore, a plot of F_{rel} vs. the log "volumes to dissolve the applied dose" (VDAD, calculated by dividing the applied dose by respective thermodynamic solubilities at pH 1, 4.5, and 7) was performed as well. A log VDAD-dependent increase in F_{rel} was observed, which again was more prominent with log VDAD at pH 4.5, followed by log VDAD at pH 7, followed by log VDAD at pH 1 (Fig. 5A–C). Sigmoidal correlations are meaningful only for pH 4.5 and 7, because for pH 1 the scatter significantly increases, probably again reflecting the *in vivo* pH in rat stomach of 3.8–5.0 [35]. F_{rel} in rat appears to be higher than 50% with log VDAD values of approximately less than −1 (pH 4.5) to −0.3 (pH 7), corresponding to a VDAD of <100 (pH 4.5) −500 (pH 7) ml/kg. Thus, assuming that F_{rel} > 50% in rats is indicative of sufficient *in vivo* dissolution in humans after oral application of solid formulations containing crystalline API (Fig. 3), drugs should exhibit a VDAD of ~100 (pH 4.5)–500 (pH 7) ml/kg or less in aqueous media to avoid insufficient or varying drug absorption due to dissolution limitation.

Interestingly, it appears that compounds need not to be completely dissolved all at once in order to be absorbed, rather always a certain percentage of the applied drug needs to be dissolved with bit by bit dissolution over time. Therefore, VDAD is an abstract value. Although the number of compounds included in the study is relatively small and experiments do not include compound-specific solubilizing effects by, e.g., cholic acid, data reveal a dependency of ADR and VDAD with corresponding relative bioavailability (reflecting *in vivo* dissolution) in rat. In contrast, an earlier study [36] could not show a correlation of log D_0 (dose strength/250 ml/solubility, [37]) and the respective fraction absorbed (reflecting *in vivo* dissolution and permeation/transport processes) of 73 compounds (orally applied as drug product). This discrepancy may be explained by the fact that D_0 values [38] given were calculated from solubilities for the uncharged, lowest solubility form reported in the Merck Index or USP [39], whereas some of the compounds may be bases and therefore completely dissolved in the human's stomach (pH 1–2). Then, following the course of the compound's GI passage, compounds may precipitate at higher pH, but still a sufficient fraction of drug be kinetically dissolved to ensure complete absorption. Also, basic compounds may precipitate in the stomach in the amorphous state, whereas D_0 values were certainly calculated from thermodynamic solubilities of crystalline compounds. The other way round, acidic compounds may well be absorbed in the intestine, although displaying poor solubility at acidic pH (24).

Interestingly, thus far it has been assumed that compounds with an aqueous solubility of less than 100 mg/L often present dissolution limitations to absorption [40,41]. Also, it has been stated that with a dose:solubility ratio (defined as the volume of gastrointestinal fluid necessary to dissolve the administered dose) of >1 L, even in the presence of favorable physiological factors (e.g., pH, bile components), the solubility would likely cause problems with respect to bioavailability [42]. According to the data presented here, both numbers (solubility <100 mg/L; dose:solubility ratio >1 L) appear to be a conservative estimate. Rather, the majority of compounds with F_{rel} of <50% in rat after p.o. application exhibit thermodynamic solubilities <10 mg/L at pH 4.5 and 7, whereas compounds with F_{rel} > 50% in rat exhibit thermodynamic solubilities of >10 mg/L at pH 4.5 and 7 (compounds 11, 15, 16 even below 10 mg/L, Table 3). Furthermore, dose:solubility ratios of compounds with F_{rel} in rat of < 50% were >20 L (dose [mg/kg] taken from Table 3 ∗ 70 kg/solubility [mg/L] at pH 4.5 and 7) at pH 4.5 and 7. Also, the mathematical model presented by Oh et al. [38] suggesting that the fraction dose absorbed has a very steep dependence on dose number (dose/solubility/volume taken with dose) and dissolution number (residence time/dissolution time) when they both have values around 1, appears to be a rather conservative approach for predicting critical solubility values that would dictate absorption limitation.

4. Conclusion

In conclusion, data presented in this study reveal ADR and VDAD needed to achieve ~50% F_{rel} in rat. Assuming that F_{rel} > 50% in rats is indicative of sufficient *in vivo* dissolution in humans after oral application of solid formulations, drugs should exhibit a VDAD of ~100 (pH 4.5)–500 (pH 7) ml/kg or less in aqueous media to avoid insufficient or varying drug absorption due to dissolution limitation. Thus, ADR and VDAD may be used to direct further chemical optimization and support *in vivo* data, altogether contributing to a successful drug development candidate.

Acknowledgements

The authors would like to thank Karl-Heinz Schlemmer, Joachim Schumacher, and Karen Engel for *in vivo* PK data; Achim Hornig for particle size measurement; Alfons Grunenberg, Gabriele Winter and Stefan Burkert for XRPD, Raman and DSC data, Gertrud Ahr for providing human clinical pharmacokinetic parameter.

References

[1] S. Venkatesh, R.A. Lipper, Role of the development scientist in compound lead selection and optimization, J. Pharm. Sci. 89 (2000) 145–154.
[2] C.A. Lipinski, F. Lombardo, B.W. Dominy, P.J. Feeney, Experimental and computational approaches to estimate solubility and permeability in drug discovery and development settings, Adv. Drug Deliv. Rev. 23 (1997) 3–25.
[3] W.N. Charman, C.J. Porter, S. Mithani, J.B. Dressman, Physiochemical and physiological mechanisms for the effects of food on drug absorption: the role of lipids and pH, J. Pharm. Sci. 86 (1997) 269–282.
[4] W.H. Moos, G.D. Green, Recent advances in the generation of molecular diversity, Annu. Rep. Med. Chem. 28 (1993) 315–324 (Chapter 33).
[5] D.V. Patel, E.M. Gordon, Applications of small molecule combinatorial chemistry to drug discovery, Drug Discov. Today 1 (1996) 134–144.

[6] P.R. Andrews, D.J. Craik, J.L. Martin, Functional group contributions to drug–receptor interactions, J. Med. Chem. 27 (1984) 1648–1657.
[7] D. Singhal, W. Curatolo, Drug polymorphism and dosage form design: a practical perspective, Adv. Drug Deliv. Rev. 56 (2004) 335–347.
[8] J.B. Dressman, C. Reppas, In vitro–in vivo correlations for lipophilic, poorly water-soluble drugs, J. Eur. Pharm. Sci. 11 (Suppl. 2) (2000) 73–80.
[9] P. Gribbon, A. Sewing, High-throughput drug discovery: what can we expect from HTS?, Drug Discov Today 10 (2005) 17–22.
[10] T. Vasconcelos, B. Sarmento, P. Costa, Solid dispersions as strategy to improve oral bioavailability of poor water soluble drugs, Drug Discov. Today 12 (2007) 1068–1075.
[11] S. Talegaonkar, A. Azeem, F.J. Ahmad, R.K. Khar, S.A. Pathan, Z.I. Khan, Microemulsions: a novel approach to enhanced drug delivery, Recent Pat. Drug Deliv. Formul. 2 (2008) 238–257.
[12] Tripos, St. Louis, MO, Biobyte Software ClogP/CRMTM.
[13] P. Ertl, B. Rohde, Fast calculation of molecular polar surface area as a sum of fragment-based contributions and its application to the prediction of drug transport properties, J. Med. Chem. 43 (2000) 3714–3717.
[14] J.C. Shelley, A. Cholleti, L.L. Frye, J.R. Greenwood, M.R. Timlin, M. Uchimaya, Epik: a software program for p*K*(a) prediction and protonation state generation for drug-like molecules, J. Comput. Aided Mol. Des. 21 (2007) 681–691.
[15] B.D. Christie, B.A. Leland, J.G. Nourse, Structure searching in chemical databases by direct lookup methods, J. Chem. Inf. Comput. Sci. 33 (1993) 545–547.
[16] OECD Guideline for the Testing of Chemicals, 107, adopted July 27 1995 (last accessed 10.08.10). <http://www.oecd.org/dataoecd/17/35/1948169.pdf>.
[17] T.J. Looney, USP Apparatus 4 (Flow-Through Method), Primer Dissolution Technologies, November 1996, pp. 10–12.
[18] F. Wunder, M.J. Gnoth, A. Geerts, D. Barufe, A. Novel, PDE2A reporter cell line: characterization of the cellular activity of PDE inhibitors, Mol. Pharm. 6 (2008) 326–336.
[19] Guidance for Industry Waiver of In Vivo Bioavailability and Bioequivalence Studies for Immediate-Release Solid Oral Dosage Forms Based on a Biopharmaceutics Classification System, U.S. Department of Health and Human Services Food and Drug Administration Center for Drug Evaluation and Research (CDER), August 2000.
[20] C. Hilgendorf, H. Spahn-Langguth, C.G. Regardh, E. Lipka, G.L. Amidon, P. Langguth, Caco-2 versus Caco-2/HT29-MTX co-cultured cell lines: permeabilities via diffusion, inside- and outside-directed carrier-mediated transport, J. Pharm. Sci. 89 (2000) 63–75.
[21] S. Yee, In vitro permeability across Caco-2 cells (colonic) can predict in vivo (small intestinal) absorption in man-fact or myth, Pharm. Res. 14 (1997) 763–766.
[22] K. Mandagere, T.N. Thompson, K.K. Hwang, Graphical model for estimating oral bioavailability of drugs in humans and other species from their Caco-2 permeability and in vitro liver enzyme metabolic stability rates, J. Med. Chem. 45 (2002) 304–311.
[23] G. Corti, F. Maestrelli, M. Cirri, N. Zerrouk, P. Mura, Development and evaluation of an in vitro method for prediction of human drug absorption. II. Demonstration of the method suitability, Eur. J. Pharm. Sci. 27 (2006) 354–362.
[24] M. Yazdanian, K. Briggs, C. Jankowsky, A. Hawi, The "high solubility" definition of the current FDA guidance on biopharmaceutical classification system may be too strict for acidic drugs, Pharm. Res. 21 (2004) 293–299.
[25] A. Corsini, T.A. Jacobson, C.M. Ballantyne, Fluvastatin: clinical and safety profile, Drugs 64 (2004) 1305–1323.
[26] L.S. Gan, P.H. Hsyu, J.F. Pritchard, D. Thakker, Mechanism of intestinal absorption of ranitidine and ondansetron: transport across Caco-2 cell monolayers, Pharm. Res. 10 (1993) 1722–1725.
[27] S. Yamashita, T. Furubayashi, M. Kataoka, T. Sakane, H. Sezaki, H. Tokuda, Optimized conditions for prediction of intestinal drug permeability using Caco-2 cells, Eur. J. Pharm. Sci. 10 (2000) 195–204.
[28] J. Keldenich, Measurement and prediction of oral absorption, Chem. Biodivers. 6 (2009) 2000–2013.
[29] S. Willmann, W. Schmitt, J. Keldenich, J. Lippert, J.B. Dressman, A physiological model for the estimation of the fraction dose absorbed in humans, J. Med. Chem. 47 (2004) 4022–4031.
[30] T. Yamagata, H. Kusuhara, M. Morishita, K. Takayama, H. Benameur, Y. Sugiyama, Improvement of the oral drug absorption of topotecan through the inhibition of intestinal xenobiotic efflux transporter, breast cancer resistance protein, by excipients, Drug Metab. Dispos. 35 (2007) 1142–1148.
[31] J. Schulze, A. Sacher, T. Backensfeld, A. Reichel, P. Lienau, In vitro and in vivo evaluation of pharmaceutical excipients: interaction potential with biological barriers, 2005 AAPS Annual Meeting and Exposition, November 2005, Nashville (M1135).
[32] B. Davies, T. Morris, Physicological parameters in laboratory animals and humans, Pharm. Res. 10 (1993) 1093–1099.
[33] T.T. Kararli, Comparison of the gastrointestinal anatomy, physiology and biochemistry of humans and commonly used laboratory animals, Biopharm. Drug Dispos. 16 (1995) 351–380.
[34] W.L. Chiou, A. Barve, Linear correlation of the fraction of oral dose absorbed of 64 drugs between humans and rat, Pharm. Res. 15 (1998) 1792–1795.
[35] E.J. Calabrese, Table 33.9, Principles of animal extrapolation, Lewis Publisher, Chelsea, MI, 1991.
[36] U. Fagerholm, Prediction of human pharmacokinetics–gastrointestinal absorption, J. Pharm. Pharmacol. 59 (2007) 905–916.
[37] J.B. Dressman, G.L. Amidon, G.L. Fleisher, Absorption potential: estimating the fraction absorbed for orally administered drugs, J. Pharm. Sci. 74 (1985) 588–589.
[38] D.-M. Oh, R.M. Curl, G.L. Amidon, Estimating the fraction dose absorbed from suspensions of poorly soluble compounds in humans: a mathematical model, Pharm. Res. 10 (1993) 264–270.
[39] N.A. Kasim, M. Whitehouse, C. Ramachandran, M. Bermejo, H. Lennernäs, A.S. Hussain, H.E. Junginger, S.A. Stavchansky, K.K. Midha, V.P. Shah, G.L. Amidon, Molecular properties of WHO essential drugs and provisional biopharmaceutical classification, Mol. Pharm. 1 (2004) 5–96.
[40] D. Hörter, J.B. Dressman, Influence of physicochemical properties on dissolution of drugs in the gastrointestinal tract, Adv. Drug Deliv. Rev. 46 (2001) 75–87.
[41] S. Balbach, C. Korn, Pharmaceutical evaluation of early development candidates; the 100 mg-approach, Int. J. Pharm. 275 (2004) 1–12.
[42] J.B. Dressman, K. Thelen, E. Jantratid, Towards quantitative prediction of oral drug absorption, Clin. Pharmacokin. 47 (2008) 655–667.